BULLETIN OF THE POLISH ACADEMY OF SCIENCES
TECHNICAL SCIENCES, Vol. 68, No. 1, 2020
DOI: 10.24425/bpasts.2020.131840

Wigner transform approach to dynamic-variable partially coherent laser beam characterization

J. JABCZYŃSKI*, P. GONTAR, and Ł. GORAJEK

Military University of Technology, Institute of Optoelectronics, 00-908 Warsaw, 2 gen. S. Kaliskiego St., Poland, www.ioe.wat.edu.pl

Abstract. 1) Background: the modeling, characterization, transformation and propagation of high-power CW laser beams in optical (including fiberoptic) trains and in the atmosphere have become hot topics in laser science and engineering in the past few years. Single-mode output is mandatory for high-power CW laser applications in the military field. Moreover, an unstationary, dynamic operation regime is typical. Recognized devices and procedures for laser-beam diagnostics could not be directly applied because of dynamic behavior and untypical non-Gaussian profiles. 2) Methods: the Wigner transform approach was proposed to characterize dynamically variable high-power CW laser beams with significant deterministic aberrations. Wavefront-sensing measurements by means of the Shack-Hartmann method and decomposition into an orthogonal Zernike basis were applied. 3) Results: deterministic aberration as a result of unstationary thermal-optic effects depending on the averaged power of the laser output was found. Beam quality determined via the Wigner approach was changed in the same way as the measurements of the beam diameter in the far field. 4) Conclusions: such an aberration component seems to be the main factor causing degradation in beam quality and in brightness of high-power CW laser beams.

Key words: laser beams, partial coherence, high-power continuous-wave lasers, Wigner transform, aberrations.

1. Introduction

High-power continuous-wave (CW) laser systems of up to 100 kW have emerged in laser laboratories and in different markets in the last two decades [1–6]. In common civilian applications (e.g. shipbuilding and the machinery industry), multimode fiber delivering is applied; thus, the beam-quality problem of the laser source is not critical. However, in military applications, the requirement of near-single-mode output is mandatory; moreover, an unstationary, dynamic regime of operation is typical. Fundamental and technical limits, 'bottlenecks', and challenges connected with the generation and delivery of such high-power CW beams to the operation point have nowadays been identified [5, 6]. Modeling, characterization, transformation and propagation of such high-power laser beams in optical (including fiberoptic) trains and in the atmosphere have now become a hot topic in laser science and engineering.

Our motivation for compiling this work was the problem of comprehensive characterization of the 10 kW class laser effector that we encountered last year [7]. We found in preliminary experiments that the ISO 11146 procedure [8] for laser-beam parameter characterization, based on the so-called 'parabolic propagation law' could not be applied directly because of untypical non-Gaussian profiles. Applying the beam quality parameter (BQP) definition as the ratio of the real beam diameter in the far field to a hypothetic diffraction-limited one (see, e.g. [4, 9]), we preliminarily characterized the output beam of our laser system for several powers and duty cycles. Moreover, the wavefront-sensing technique enabled us to register aberrated wavefronts of such beams; thus, we obtained two sets of complimentary experimental data: beam-size measurements in the far field, and wavefront measurements.

The main finding was that BQP is a dynamic variable that significantly degrades with averaged laser power. We supposed that the deterministic component of wavefront aberrations, caused by dynamic thermo-optic phenomena occurring inside the laser system, played an important role here [10–12]. Thus, we decided to develop analytic/experimental tools to verify that hypothesis.

The aim of the paper was to develop experimental and theoretical tools for the characterization of such dynamically variable partially coherent laser beams having a significant deterministic aberration component. Such a beam can be described in first-step approximation as a partially coherent **G**aussian-**S**chell beam with an additional **D**eterministic **A**berration component (GSDA beam). We briefly describe the analytical model of such a beam based on the Wigner transform approach in Section 2. In the following section, the experiment setup is described, and then measurement results are presented and discussed.

2. Methods

2.1. Wigner transform approach. Wigner transform was proposed by M.J. Bastiaans [13] as well as R. Simon, N. Mukunda and E. Sudarshan [14] for the analysis of partially coherent beams in wave optics in the 1980s. Wigner distribution (WD), in brief, is the Fourier transform of a partial coherence function with respect to correlation coordinates. In WD, we simultane-

*e-mail: jan.jabczynski@wat.edu.pl

Manuscript submitted 2019-08-13, revised 2019-12-04, initially accepted for publication 2019-12-04, published in February 2020

ously have access to the beam shape in the near field as well as the beam profile in the far field. This excellent idea was accepted and became widespread (see, e.g. [15–18]) in laser optics in the last two decades. A very interesting result was the possibility to analyze the impact of geometric aberrations [16, 18] on Wigner distribution. Moreover, B. Eppich proposed the inverse procedure [16] that enabled to determine WD and the resulting Poynting vector and wavefront distortions, when knowing the experiment data of beam profiles registered in several sections in the vicinity of caustics.

2.1.1. GSDA beam model. Let us assume radial symmetry for the beam profile and wavefront distortion. Analysis can be limited to a 2D subspace of Wigner distribution $WD\ (\rho, \theta_r)$. We propose the analytical model of Wigner distribution for a **G**aussian-**S**chell beam completed with **D**eterministic **A**berrations [16,18], as follows:

$$WD_{GSDA}(\rho, \theta_r) = \exp\left[-2\left(\frac{\rho}{w_0 m_{pc}}\right)^2 - 2\left(\frac{\theta_r - W_{ray}(\rho)}{\theta_0 m_{pc}}\right)^2\right] \quad (1)$$

where ρ, θ_r – coordinates in the near and far field, respectively, in Wigner space; w_0, θ_0 – beam radii in the near and far field, respectively; m_{pc} – partial coherence parameter; and $W_{ray}(\rho)$ – ray aberration, defined as follows:

$$W_{ray}(\rho) = \nabla_\rho W_{npar,\,wave} = \frac{\partial W_{npar,\,wave}}{\partial \rho} \quad (2)$$

where $W_{npar,\,wave}$ – nonparaxial component of wave aberration function. We assume here the ray aberration/direction W_{ray} given from theory (p. 2.1.3, Fig. 2) or experiment (p. 3) wave aberration (formula (2)) and 'spread' it by a priori defined beam divergence width $\theta_{0*}m_{\mathrm{pc}}$. The work out and physical proof of that approach will be provided in our next paper.

Knowing any distribution in Wigner space (e.g. $WD_{GSDA}(\rho, \theta_r)$), we can transform it into a physical space (r_n, α) by applying Radon transform $\Re$ [16, 18] (see Fig. 1)

$$\begin{aligned} &I_n(r_n, \alpha) = \Re\left[WD(\rho, \theta_r)\right] \\ &\rho \to r_n = \rho/\cos(\alpha); \quad \theta_r \to \alpha = arctg(\rho/\theta_r) \end{aligned} \quad (3)$$

where $r_n = r/w(\alpha)$ is the normalized radius-distance to the axis, $w(\alpha)$ is the beam radius at distance z corresponding to angle α between r axis and point (r, α_r) in WD, equal to a Gouy phase-shift angle, and Z_R is the Rayleigh range as follows:

The 2D map of WD in Wigner space (Fig. 1a) corresponds to the 2D map of normalized intensity $I_n(r_n, \alpha)$ in space (r_n, α) (Fig. 1b) and to the 2D intensity map determined in physical coordinates $(r, z/Z_R$; Fig. 1c).

2.1.2. Beam quality metrics. Following the results of [16, 18], we had the direct possibility to determine several beam-quality metrics (see, e.g. [19]) applying averaging over 2D Wigner distribution.

The $M_{WD}{}^2$ parameter of such a beam can be defined as follows [14, 16]:

$$M_{WD}{}^2 = \sqrt{\left\langle\rho^2\right\rangle\left\langle\theta^2\right\rangle - \left\langle\theta\rho\right\rangle^2} \quad (4)$$

where:

$$\begin{aligned} \left\langle\rho^2\right\rangle &= 4P_0^{-1}\iint \rho^2 WD(\rho, \theta)\,d\rho d\theta \\ \left\langle\theta^2\right\rangle &= 4P_0^{-1}\iint \theta^2 WD(\rho, \theta)\,d\rho d\theta \\ \left\langle\theta\rho\right\rangle &= 4P_0^{-1}\iint \theta\rho WD(\rho, \theta)\,d\rho d\theta \\ P_0 &= \iint WD(\rho, \theta)\,d\rho d\theta \end{aligned} \quad (5)$$

The $M_{WD}{}^2$ parameter defined in such a manner is equivalent to the definition of Siegman's beam-propagation factor [20]. Let us notice that the $M_{WD}{}^2$ parameter has a global character and is not directly equivalent to experiment results performed according to the ISO 11146 procedure. In some cases, different beam-quality metrics are important, especially the beam quality parameter [4, 9, 19], defined as the ratio of the beam diameter in the far field to a hypothetical diffraction-limited beam size.

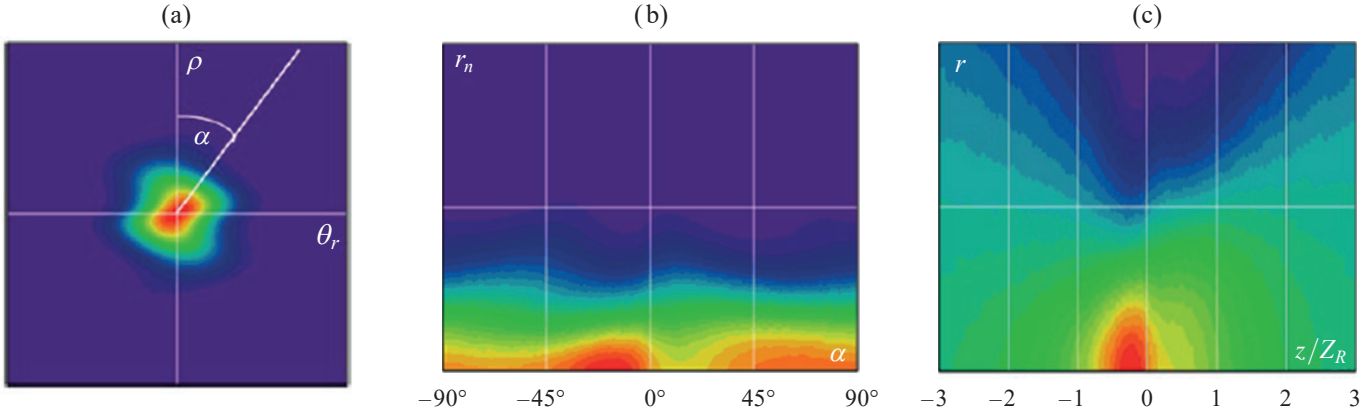

Fig. 1. a) 2D map of Wigner distribution (WD) in Wigner space (r, θ_r), b) 2D map of normalized intensity in space (r_n, α), c) 2D map of normalized intensity in physical space $(r, z/Z_R)$

In the case of the WD_{GSDA} model, the diffraction-limited beam is the aberration-free fully coherent beam ($m_{pc} = 1$, $W_{ray} = 0$) shown in Fig. 3, Case 1, which has both second moments $\langle \rho^2 \rangle = \langle \theta^2 \rangle = 1$. We propose to introduce the following definition of BQP_{WD}:

$$BQP_{WD} = \sqrt{\langle \theta^2 \rangle}. \tag{6}$$

Beam sizes in the near and far field can change as a result of aberration and partial coherence. The complimentary parameter characterizing the influence of both effects is normalized brightness $B_{nor,\,WD}$, defined as follows:

$$B_{nor,\,WD} = \frac{1}{\langle x^2 \rangle \langle \theta^2 \rangle} \tag{7}$$

Definite ray-aberration data can be taken from modeling (see Section 2.2) or wavefront measurements (see Section 3).

2.1.3. GSDA for thermo-optic aberration determined in modeling. WD describes spatial properties of any partially coherent beam in a comprehensive manner, and can be treated as the 'fingerprints' of the examined beam, showing partially coherent and aberrated properties. To introduce and better understand the physical sense of the Wigner approach, let us examine the properties of a partially coherent beam having an a priori determined aberration (shown in Fig. 2) taken from the thermo-optic model of a laser mirror under a high heat load [12].

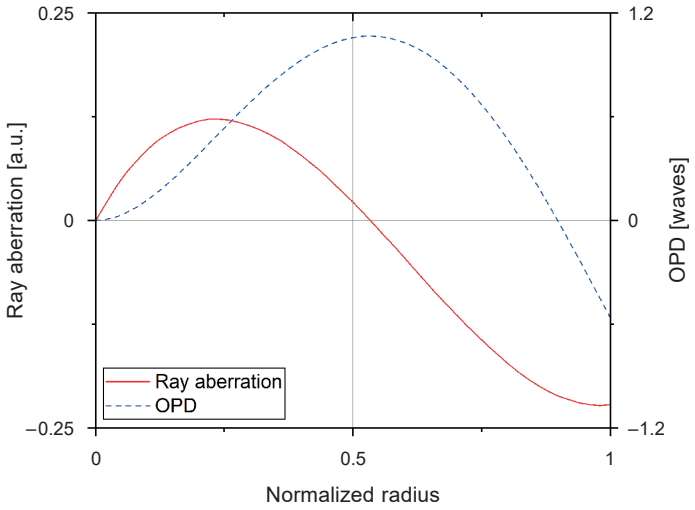

Fig. 2. Thermal-optic aberration vs. radius: wave aberration [12] (blue-dashed) and ray aberration (red)

We have calculated four possible cases of WD_{GSDA}. Results are summarized in Table 1 and Fig. 3. Case 1 corresponds to

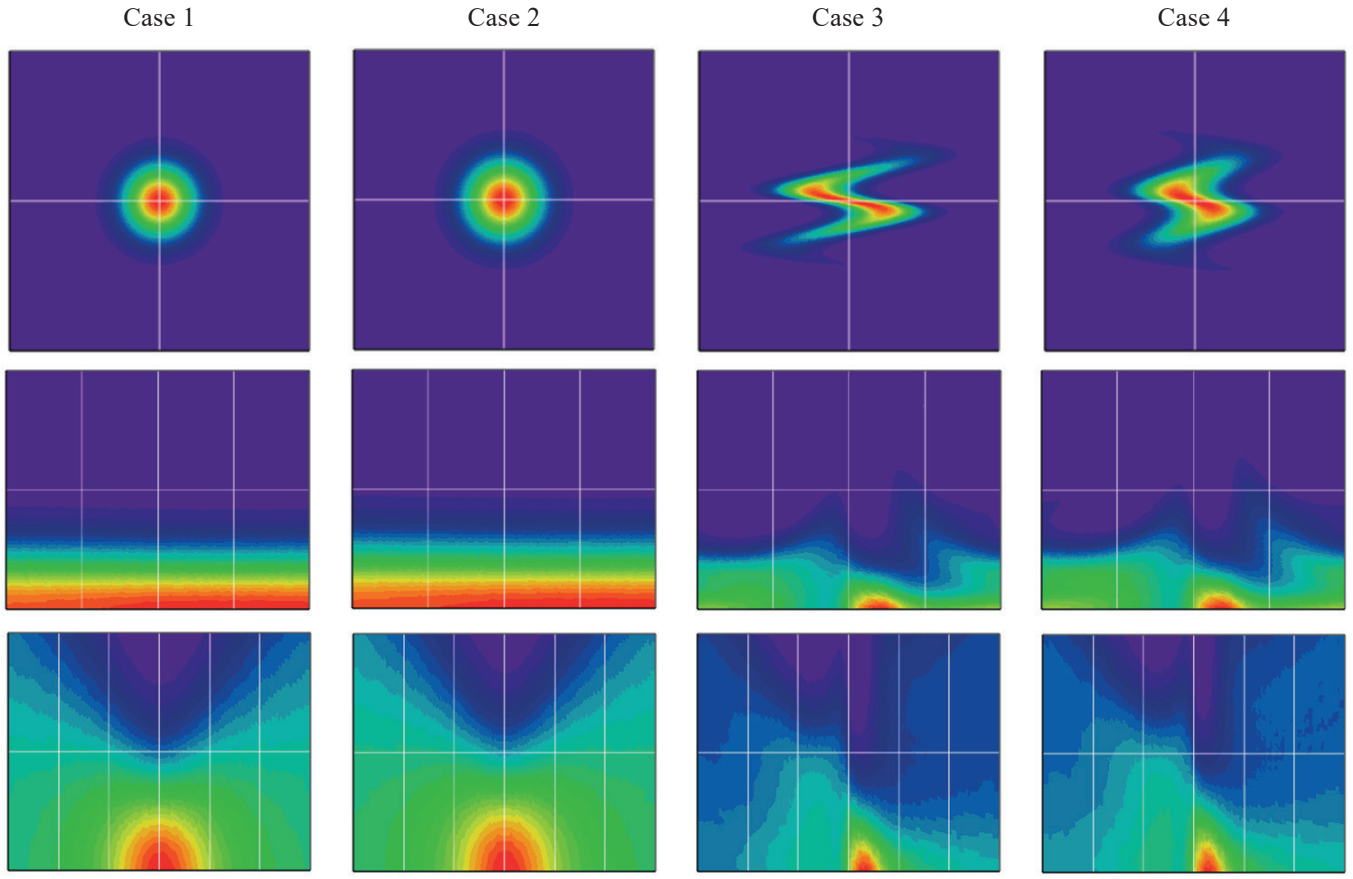

Fig. 3. Two-dimensional maps of WD (first row), normalized intensity (second row), and intensity in physical space (last row)

Table 1
Results of beam-quality metrics calculations for thermal-optic aberration, taken from [12]

case No	1	2	3	4
m_{pc}	1	1.096	1	1.096
rmsOPD	0	0	0.39	0.39
BQP_{WD}	1	1.095	1.216	1.321
$M_{WD}{}^2$	1	1.2	1.2	1.414
$B_{nor,\,WD}$	1	0.694	0.685	0.493

the diffraction-limited beam ($m_{pc} = 1$), while Case 2 corresponds to a partially coherent beam ($m_{pc} = 1.096$) without deterministic aberration. In the two latter cases, we took the ray aberration, shown in Fig. 2, for a fully coherent beam (Case 3; $m_{pc} = 1$) and for a partially coherent beam (Case 4; $m_{pc} = 1.096$).

Note that such an approach enables the visualization of defocusing, beam spreading, untypical non-Gaussian profiles, and the qualitative analysis of wavefront-aberration and spatial-coherence effects on beam-quality metrics.

2.2. Experimental setup. The experimental part of this work aimed at developing a specific measurement method and setup for high-power CW laser source characterization performed in a comprehensive manner. A brief description of the laboratory setup is provided below.

After passing through a long focal length lens, the high-power CW laser beam is attenuated in a series of Fresnel reflections on uncoated optical wedges.

The final steady state, reached for our laser source in up to dozens of minutes, was beyond the scope of our interest. Our aim was to monitor the dynamic behavior of a laser beam in a scale from parts of seconds up to a few dozen seconds. The main experimental problem consisted of dynamic changes in beam size and locations due to the increasing thermal load inside the laser system (deterministic component) as well as additional laboratory noises and turbulence inside the measurement setup. Typical laser-beam diagnostic devices (e.g. PRIMES LQM and Ophir ModeScan) require relatively long time for measurements (even up to a few minutes) because of beam scanning along the caustics needed in the ISO 11146 procedure. We have found in preliminary experiments that such a method renders erroneous results, especially for higher CW powers, because of untypical non-Gaussian profiles and the dynamic variable during the measurement-process properties of the laser beam itself. Thus, a measurement method and device as close as possible to a 'single-shot' regime were both required.

We used two alternative and complimentary diagnostic methods and devices:

– Direct measurement of beam size in the far field via a large 2D area frame; CMOS camera JAI SP-20000-USB Mono.
– Wavefront-Sensing Measurement (WSM) via a Thorlabs Wavefront Sensor based on Hartmann–Shack Test WFS150.

In the first case, acquisition time of a few tens of milliseconds is possible, whereas measurement time with wavefront calculation amounted to parts of a second in the latter case. Note that, in principle, WSM is achromatic and non-sensitive to polarization, a coherence state, and the 'single-shot' method (see, e.g. [21]) because we have access to the wavefront and to the beam profile (proportional to local intensities-power in the subaperture) for a single exposition. However, to obtain reliable results with an acceptable S/N ratio, the average from a series of expositions has to be taken. Because of the technological limit, the number of subapertures is a few dozen in one dimension. Thus, we have much lower lateral resolution when compared to typical laser-beam profiles based on CCD or CMOS cameras. On the other hand, we have access to the 2D shape of the wavefront with a resolution of a few tens of nm. With the Wigner approach and GSDA beam model, we can characterize the laser beam being examined in a comprehensive manner. Beam radius w_0 and the ray aberrations needed to perform calculations were taken from WSM measurements. We limited this to the fifth-order Zernike's orthogonal basis of polynomials for wavefront approximation in preliminary calculations. After removing the parabolic part, ray aberration was determined (see Fig. 5) and, following the 2D maps, WD and intensities were calculated (see Fig. 6).

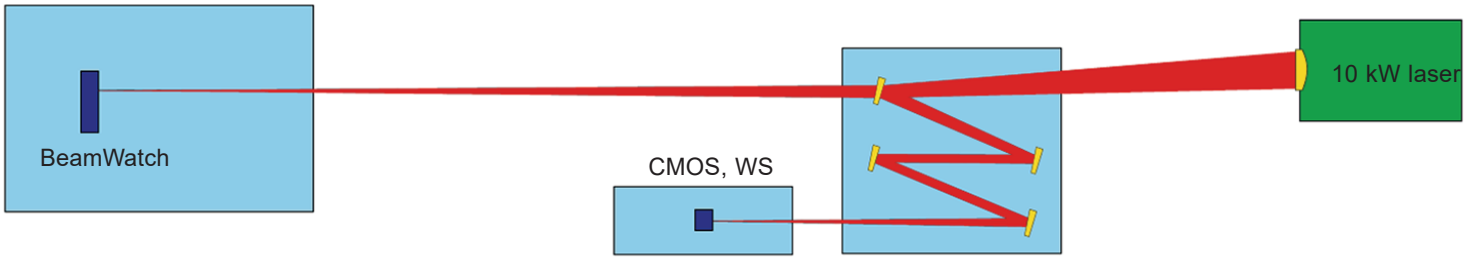

Fig. 4. Scheme of laboratory setup

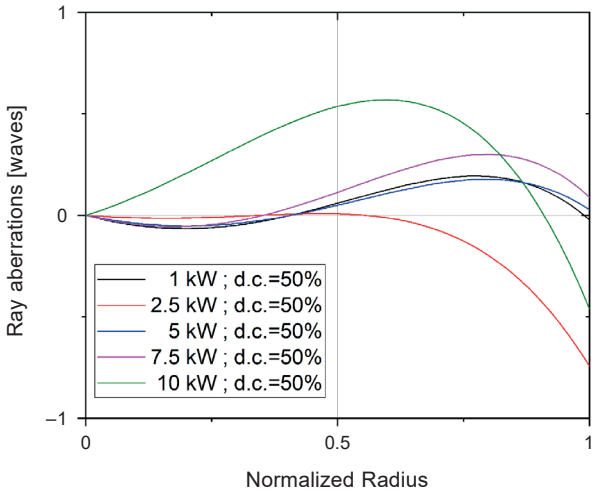

Fig. 5. Ray aberrations vs. radius for several powers; d.c. = 50%

3. Results

To test the method, we used the 50% duty-cycle (d.c.) regime (10 ms pulse duration and 20 ms period). For such a regime, the laser beam was directly recorded in the far field by the CMOS camera and by the WSM. Results were presented in Fig. 5 and Fig. 6.

Having determined the WD_{GSDA} for a set of powers and the d.c., we calculated the beam quality parameter and brightness according to the definitions provided in Section 2 (see Fig. 7 and Fig. 8).

4. Discussion

The existence of a variable with an averaged-power thermal-optic aberration was proven in the experiments. More-

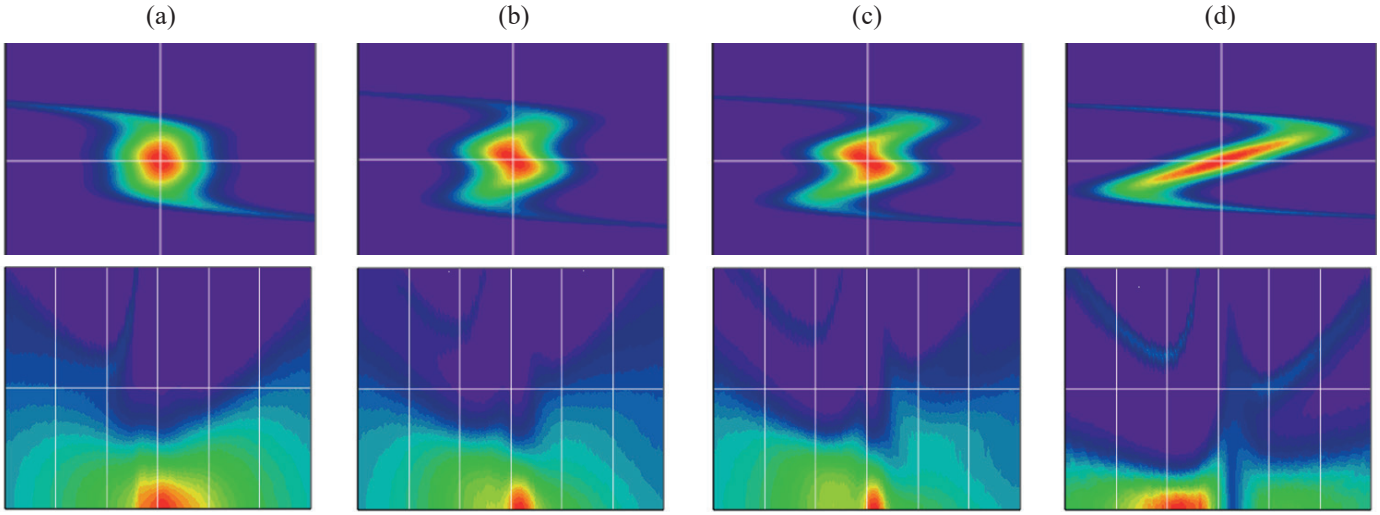

Fig. 6. a) WD and intensity @ 2 kW, d.c = 50%, b) WD and intensity @ 5 kW, d.c = 50%, c) WD and intensity @ 7.5 kW, d.c = 50%, (d) WD and intensity @ 10 kW, d.c. = 50%

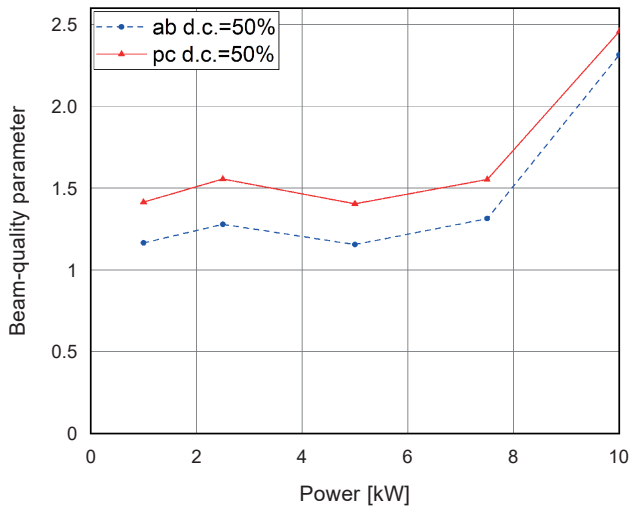

Fig. 7. Beam-quality parameter vs. power. Aberration + partial coherence—continuous line; aberration – dashed line

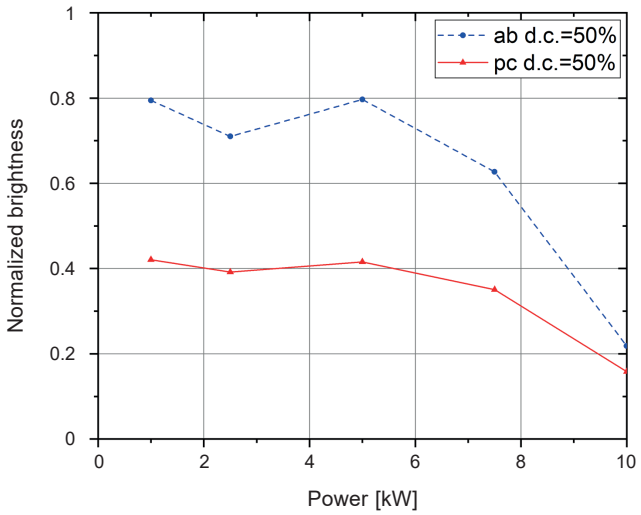

Fig. 8. Normalized brightness vs. power. Aberration and partial coherence—continuous line; aberration – dashed line

over, the reasons for the untypical non-Gaussian profiles were explained by analyzing the WD and resulting 2D intensity maps in the caustics. Similar results were obtained applying the ABCD Fresnel transformation for the coherent beam of Gaussian profile and taken from WSM wave aberration. Beam quality, determined via the Wigner approach, was changed in the same manner as the measurements of the beam diameter in the far field. The model of thermal-optic aberration (Section 2.1.3) was in qualitative accordance with the experiment results obtained via wavefront-sensing measurements.

The parameters of our measurement setup were satisfactory for the preliminary estimation of physical effects. After enhancement and modification, such a procedure can be used in the comprehensive characterization of our 10 kW class laser effector and its modernized versions in the future.

5. Conclusions

A thermal-optic aberration component seems to be the main factor causing degradation in beam quality and in brightness of high-power CW laser beams. Such information could become the basis for arguments to modify/improve beam-forming optics or to apply the method of adaptive optics to correct those distortions (see, e.g. [4]). Both the method and application used for such a specific task could be interesting for a wide group of laser physicists and engineers working in that area of laser engineering.

Acknowledgements. The work was financed within the framework of strategic program DOB-1–6/1/PS/2014, financed by the National Center for Research and Development, Poland. We would like to thanks Z. Zawadzki, PhD, for the discussion on Wigner transform.

References

[1] S.J. McNaught, H. Komine, S.B. Weiss, R. Simpson, A.M. Johnson, J. Machan, C.P. Asman, M. Weber, G.C. Jones, M.M. Valley, A. Jankevics, D. Burchman, M. McClellan, J. Sollee, J.Marmo, and H. Injeyan, "100 kW Coherently Combined Slab MOPAs", in *Conference on Lasers and Electro-Optics/International Quantum Electronics Conference, OSA Technical Digest* (CD), paper CThA1 (2009).

[2] Z. Mierczyk, "Lasers in the dual use technologies", *Bull. Pol. Ac.: Tech.*, 60(3), 691–696 (2012).

[3] J. Badziak, "Laser nuclear fusion: current status, challenges and prospect", *Bull. Pol. Ac.: Tech.*, 60(4), 729–738 (2012).

[4] L. Sun, Y. Guo, C. Shao, Y. Li, Y. Zheng, C. Sun, X. Wang, and L. Huang, "10.8 kW, 2.6 times diffraction limited laser based on a continuous wave Nd:YAG oscillator and an extra-cavity adaptive optics system", *Opt. Lett.*, 43(17), 4160 – 4163 (2018).

[5] H. Injeyan, S. Palese, and G.D. Goodno (*High Power Laser Handbook*, Mc Graw Hill, New York, 2011).

[6] R.A. Motes, S.A. Shakir, and R.W. Berdine, *Introduction to High Power lasers*, (Directed Energy Professional Society, Albuquerque NM, USA, 2013).

[7] P. Gontar, L. Gorajek, K. Kopczyński, and J.K. Jabczyński, "Characterization of beam quality of 10-kW class laser demonstrator", *Proc. SPIE*, 11624–4 (2019).

[8] *ISO/TR 11146–3*, *Lasers and laser-related equipment- Test methods for laser beam widths*, *divergence angles and beam propagation ratios – Part 3: Intrinsic and geometrical laser beam classification*, *propagation and details of test methods*, ISO, (2004).

[9] J. Marmo, H. Injeyan, H. Komine, S. McNaught, and J. Machan, "Joint high power solid state laser program advancements at Northrop Grumman", *Proc. SPIE*, 7195, 719507 (2009).

[10] J. Penano, P. Sprangle, A. Ting, R. Fischer, B. Hafizi, and P. Serafim, "Optical quality of high-power laser beams in lenses", *J. Opt. Soc. Am. B*, 26(3), 503–510 (2009).

[11] B. Fakizi, A. Ting, D.F. Gordon, P. Sprangle, J.R. Penano, R.F. Fischer, G. DiComo, and D.C. Colombant, "Laser heating of uncoated optics in a convective medium", *Appl. Opt.* 51(14), 2573–2580 (2012).

[12] J.K. Jabczynski, M. Kaskow, L. Gorajek, K. Kopczynski, and W. Zendzian, "Modeling of the laser beam shape for high-power applications", *Opt. Eng*. 57(4) 046107 (2018).

[13] M.J. Bastiaans, "Application of the Wigner Distribution Function", *J. Opt. Soc. Am. A*, 3, 1227 (1986).

[14] R. Simon, N. Mukunda, and E.C.G. Sudarshan, "Partially coherent beams and a generalized ABCD law", *Opt. Comm.*, 65, 322–328 (1988).

[15] M.A. Alonso, "Wigner functions in optics: describing beams as rays bundles and pulses as a particle ensemebles", *Advances in Optics and Photonics*, 271–365 (2011).

[16] B. Eppich, S. Johansson, H. Laabs, and H. Weber, "Measuring laser beam parameters, phase and spatial coherence using the Wigner function", *Proc. SPIE*, 3930, 76–86 (2000).

[17] B. Eppich, G. Mann, and H. Weber, "Spatial coherence: comparison of interferometric and non-interferometric measurements", *Proc. SPIE*, 4969–37 (2003).

[18] B.J. Neubert, *Measurements of the Wigner Distribution of Aberrated and Partially Coherent Laser Beams* , PhD thesis, Cuvillier Verlag Goettingen, Germany, 2004.

[19] T. Sean Ross, *Laser Beam Quality Metrics*,(SPIE Press, Bellingham, USA, 2013).

[20] A.E. Siegman, "New Developments in laser resonators", *Proc. SPIE*, 1224, 2–14 (1990).

[21] *Handbook of Optical Systems: Vol. 5. Metrology of Optical Components and Systems*., *Non-interferometric Wavefront Sensing*. Edited by Herbert Gross, (Wiley-VCH Verlag GmbH, Chapter 47 2012).